Journal of Current Science and Technology, September - December 2023 Vol. 13 No. 3, pp. 574-583

ISSN 2630-0656 (Online)
Cite this article: Thaweekhotr, P., Thongsopha, C., Sudwan, P., Bumroongkit, K. Seeharach, K., Jaiyen, C., Suannahoy, P., Phasukdee, N., Quiggins, R. (2023). Histological features of cerebral arteries and brain parenchyma in cadavers who had died from hemorrhagic stroke. *Journal of Current Science and Technology*, *13*(3), 574-583. https://doi.org/10.59796/jcst.V13N3.2023.768

Journal of Current Science and Technology

Journal homepage: https://jcst.rsu.ac.th

Histological Features of Cerebral Arteries and Brain Parenchyma in Cadavers Who Had Died from Hemorrhagic Stroke

Pornnarez Thaweekhotr[1, 2, 3], Chanida Thongsopha[1], Paiwan Sudwan[1], Kanokkan Bumroongkit[1], Kewalee Seeharach[1], Chatchadaporn Jaiyen[1], Patipath Suannahoy[1], Noppadol Phasukdee[1] and Ranida Quiggins[1*]

[1]Department of Anatomy, Faculty of Medicine, Chiang Mai University, Chiang Mai 50200, Thailand
[2]Graduate School, Chiang Mai University, Chiang Mai 50200, Thailand
[3]School of Integrative Medicine, Mae Fah Luang University, Chiang Rai 57100, Thailand

*Corresponding author; Email: ranida.quiggins@cmu.ac.th

Received 14 March, 2023; Revised 20 May, 2023; Accepted 1 June, 2023;
Published online 30 August, 2023

Abstract

Cerebral atherosclerosis is a risk factor for stroke. Several contents in the atheromatous plaque have been identified, but some have not yet been quantified. This is especially true for lipids. This study aims to compare the histology, vascular wall contents of the cerebral artery ipsilateral to the hemorrhagic lesion, and hemorrhagic parenchyma to that of the contralateral and the control. The A1, M1, and P1 segments of cerebral arteries from twelve stroke cadavers and those from eight control cadavers were used in this study. All segments were prepared for H&E, Sudan black B, trichrome, and modified Verhoeff's Van Gieson stains and were then analyzed for vascular parameters, lipid area, collagen area, and elastic density, respectively. The results show that the wall areas of A1 and P1 ipsilateral to hemorrhagic lesions were significantly larger than those of the contralateral. The areas of the vascular lumen of M1 ipsilateral and contralateral to the hemorrhagic lesion were significantly smaller than that of the control. The largest lipid area was found in the ipsilateral M1 among the three groups. The collagen area in the ipsilateral M1 was significantly larger than that of the control. Finally, the elastic fibers in all ipsilateral segments had significantly less density than that of the control. The nervous parenchyma contralateral to the hemorrhage was shown to be an impaired tissue. In conclusion, high accumulations of lipids and collagen, along with low elastic density in the ipsilateral M1, might have reduced the size of its lumen and its flexibility, potentially resulting in a hypertensive hemorrhage.

Keywords**:** *cadaver; cerebral artery; cerebral hemorrhage; atherosclerosis; vascular wall content; vascular parameter*

1. Introduction

Stroke is one of the top five causes of death in Northern Thailand (Thaweekhotr et al., 2022). Hemorrhagic stroke makes up about 93 percent of stroke cadavers. Atherosclerosis is one of the most common causes of cerebrovascular disease (Chandra et al., 2017). Atherosclerotic plaque found in the intracranial artery was found to be related to vascular risk factors (Gorelick, Wong, Bae and Pandey, 2008). Incidences of intracranial atherosclerosis are higher in Asian populations than in Caucasian ones (Kim, Kang and Kwon, 2005). It is commonly found in the anterior cerebral circulation, and most likely in the middle cerebral artery (Yang et al., 2017). Atherosclerosis found in the extraparenchymal large vessel was presented in the hypertensive hemorrhagic brain (Pleşea et al., 2005). Atheromatous plaque was found in the

cerebral arteries of the elderly who had died from stroke and other conditions (Enache et al., 2012). This plaque consists of a fibrous cap, a necrotic lipid-rich core, and a migrated smooth muscle (Chandra et al., 2017). These results revealed the presence of both vascular walls thickening and vascular lumen narrowing. Conventional Hematoxylin and Eosin staining was used to identify the atheromatous plaque found in the cerebral artery, while Goldner-Szekely trichrome and Orcein staining were used to differentiate the collagen fibers, smooth muscle cells, and elastic fibers in the plaque, respectively (Enache et al., 2012). The lipid in the plaque was poorly stained using those techniques. The lipid in that tissue could be better viewed by Sudan black B staining (Gerrits et al., 1992). The histological characteristics of intracranial atherosclerosis of the Chinese postmortem have been reported using conventional routine staining but these did not identify the component of the atheromatous plaque (Yang et al., 2017).

Our previous study in stroke cadavers reported that hemorrhagic lesions in the cerebral hemisphere usually occurred in the vascular territory of the cortical branches of the middle, posterior, and anterior cerebral arteries, respectively (Thaweekhotr et al., 2022). In this study, we were interested in the histological and content changes of these cerebral arteries and brain parenchyma ipsilateral to the hemorrhagic hemisphere compared to those of the contralateral using the same hemorrhagic brains used for a previous study.

2. Objective

To evaluate the histological changes of the extraparenchymal cerebral artery and parenchyma; and quantitatively determine the contents in the cerebral arteries of cadavers who had died by hemorrhagic stroke housed at The Department of Anatomy, Faculty of Medicine, Chiang Mai University.

3. Materials and methods

3.1 Sample preparation

A total of 20 cadaveric brains (12 hemorrhagic and 8 control) were used in this study. Twelve hemorrhagic brains were from cadavers aged between 38 and 79 years; 60 ± 12 years including 6 brains that had stroke occurring in both hemispheres (S620801, S620802, S620901, S630303, S630701, and S630801), two brains showed stroke in the left hemisphere (S630302 and S630302), and four brains had evidence of stroke in the right hemisphere (S621901, S621101, S630301, and S601107). Eight control brains were collected from cadavers aged from 62 to 81 years old; 72 ± 7 years where death occurred from non-cerebrovascular disease (C610401, C620901, C630301, C630901, C630902, C631001, C631101, and C640201). The A1 segment of the anterior cerebral artery (ACA), M1 segment of the middle cerebral artery (MCA), and P1 segment of the posterior cerebral artery (PCA) of the hemorrhagic brains and those of the normal brains were used for study. The A1 segment is the vascular portion originating from the internal carotid artery and extends to the anterior communication artery and the M1 segment is the vascular portion originating from the carotid bifurcation to where branching reaches the temporal and insula lobes (Chandra, et al., 2017). The P1 segment is the vascular portion occurring from the termination of the basilar artery and extends to the posterior communicating artery (Javed, Reddy, & Das, 2022). All vascular segments were divided into 3 groups according to hemorrhagic hemispherical side; ipsilateral (n = 18), contralateral (n = 6), and control vessels (n = 16). Moreover, approximately 1.0 x 1.0 x 0.7 cm^3 brain tissue blocks at the hemorrhagic region and of the symmetry region in the contralateral hemisphere were collected.

All arterial segments and blocks of brain tissue were fixed in 10% formalin solution for over 24 hours. The vessels were cross-sectioned at a 20 µm thickness using a cryostat (Leica CM1850). The six alternative sections of A1, M1, and P1 segments were collected and mounted on gelatin coated glass slides for one staining technique. Four sets of those tissue slides were prepared for Hematoxylin and Eosin, Sudan black B, Trichrome, and Elastic staining techniques, respectively. The fixative brain tissue was sectioned to a thickness of 50 µm.

3.2 Hematoxylin and Eosin (H&E) staining

The slides of A1, M1, and P1 and those of brain tissue were stained using H&E Stain Kit (ab245880; Abcam, Cambridge, MA, USA). The collagen and muscle fibers of vessels were stained in a pink color. The H&E-stained vessels were evaluated for structural changes including the perimeter of the vascular lumen, area of the vascular wall, and area of vascular lumen. The H&E-stained

brain tissues of the ipsilateral and contralateral hemorrhagic hemispheres were compared.

3.3 Sudan black B (SBB) staining

The sections of A1, M1, and P1 were stained using Sudan black B, a fat-soluble diazo dye (ab146284; Abcam, Cambridge, MA, USA). All tissue slides were incubated in a solution of 0.7 g SBB in 100 ml of 70% alcohol for 60 minutes. The lipid in the vascular wall was stained black while the rest remained colorless. After that, the vascular tissue was counterstained with hematoxylin for 15 seconds to review the other cells and connective tissue.

3.4 Trichrome (TRI) staining

The slides of A1, M1, and P1 were stained using a Trichrome Stain Kit (ab150686; Abcam, Cambridge, MA, USA) to detect the collagen and muscle fibers of vessels. All slides were incubated in a preheated Bouin's fluid for 60 minutes. After rinsing in water, the slides were transferred into the Weigert's Iron Hematoxylin for 10 minutes and then rinsed in water. The slides were incubated in a Biebrich Scarlet solution for 60 seconds. After rinsing in water, the slides were placed in a phosphomolybdic/phosphotungstic acid solution until the collagen was colorless. Next, the slides were incubated in an Aniline Blue solution for 60 seconds until the collagen had turned blue and muscle fibers had turned red.

3.5 Elastic Verhoeff Van Gieson (EVG) staining

The slides of A1, M1, and P1 were stained for detecting the elastic fibers using an Elastic Stain Kit ab150667 (ab150667; Abcam, Cambridge, MA, USA) or a modified Verhoeff's Van Gieson/ EVG stain. All slides were incubated in a Verhoeff's hematoxylin solution for 20 minutes. After rinsing with water, the tissue sections were differentiated in 2% Ferric Chloride solution and then were counterstained with a Van Gieson's solution for 15 seconds. The elastic, muscle, and collagen fibers were stained black, yellow, and red, respectively. After each staining process was completed, all slides were rinsed in tap water, dehydrated through graded alcohol, cleared with xylene, and then cover-slipped.

3.6 Procedure of measurement

All stained vascular sections from all stained methods were investigated under a light microscope and were photographed by setting at: Normal mode; Scale 2x; Resolution quality 2,560 x 1,920 pixels; Manual exposure 1/250s and gain 1.00x; and anti-reflex contrast & auto-white color. The photographs were imported into the ImageJ software for quantitative measurements.

The structural changes, including the perimeter of the vascular lumen, area of the vascular wall, and area of the vascular lumen were evaluated using the H&E-stained vessels. The lipid and collagen areas in the vascular wall were evaluated from the SBB- and TRI- stained vessels, respectively. The relative density of the internal elastic lamina was analyzed from the EVG-stained vessels. The internal elastic lamina surrounding the vascular lumen was selected for evaluating its relative density. The stained elastic fibers were reviewed in black color. The color intensity of the internal elastic laminar was analyzed using a numeric value with the red-green-blue color (RGB) model of the ImageJ software which varied between 0 to 255. The darkest black represented the highest internal elastic lamina which was represented by the numeric value of 0, while the lightest black represented the numeric value of 255.

3.7 Statistical data analysis

The quantitative data were shown as mean ± SD. To compare the data among 3 groups (ipsilateral, contralateral, and control vessels) the level of distribution was determined. One-way analysis of variance (ANOVA) was analyzed at a point when the data had a normal distribution. Kruskal-Wallis H test was applied when the data had an abnormal distribution. The p values < 0.05 were considered statistically significant when compared with control.

3.8 Ethics

This research was approved by the Ethical Review Committee for Research in Human Subjects, Faculty of Medicine, Chiang Mai University (CMU) (No. Exemption-6589/2562).

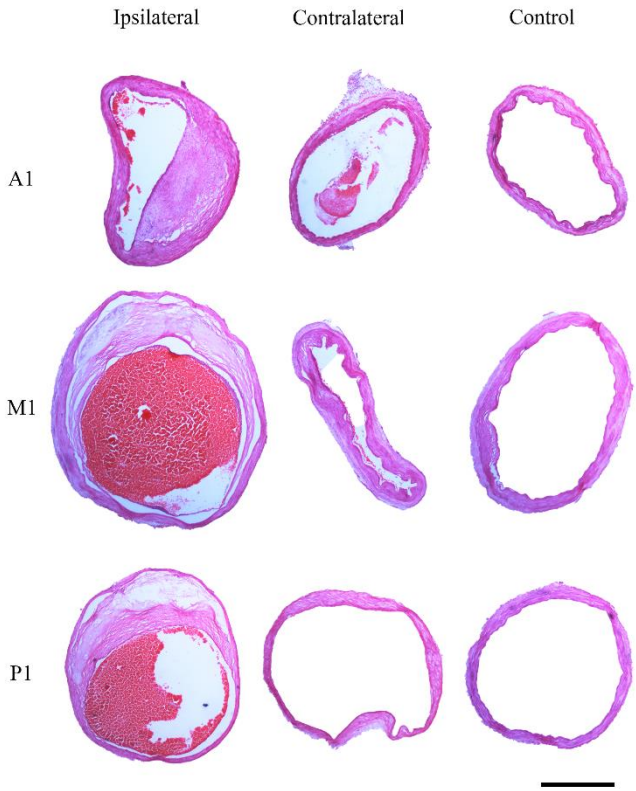

Figure 1 The hematoxylin and eosin-stained cross-sectional vessels of the A1 (S630702), M1 (S630801), and P1 (S630702) ipsilateral to hemorrhage and the A1 (S621001), M1 (S631101), and P1 (S630302) contralateral to hemorrhage, and that of the control A1 (C630901), M1 (C630902), and P1 (C630901). The scale bar is 1 mm.

4. Results

4.1 Morphological changes in hemorrhagic cerebral artery

All ipsilateral hemorrhagic vessels demonstrated irregular thickness while those of the contralateral hemorrhagic and the control vessels displayed regular wall thicknesses, as shown in Figure 1. There were empty areas within the thickened region of the ipsilateral A1, M1, and Pl. The contours of the ipsilateral and contralateral hemorrhagic vessels were distorted. A blood clot was also found in the lumen of the ipsilateral hemorrhagic M1 and P1.

The vascular parameter, being the luminal perimeter, the wall area, and the luminal area of the ipsilateral A1, M1, and P1, were compared to those of the contralateral and the control as shown in Table 1. The luminal perimeter of the ipsilateral and the contralateral A1, M1, and P1 were not significantly different when compared to the control. The cross-sectional area of the wall of the ipsilateral A1 (2.39 ± 1.6 mm^2) was significantly larger than that of the control (1.72 ± 0.74 mm^2) and these areas of the ipsilateral A1 (2.39 ± 1.6 mm^2) and P1 (3.16 ± 1.96 mm^2) were larger than the corresponding contralateral vessels (1.42 ± 0.43 mm^2) and (2.22 ± 1.8 mm^2), respectively. Interestingly, there was no difference between the luminal area of the ipsilateral (3.02 ± 2.17 mm^2) and the contralateral (2.04 ± 1 mm^2) M1. These areas were significantly smaller than the control M1 (5.6 ± 1.44 mm^2).

Table 1 The vascular parameters of the ipsilateral and contralateral A1, M1, and P1 in hemorrhagic stroked cadavers and those of the control.

Parameter	Ipsilateral	Contralateral	Control
1. Luminal perimeter (mm)			
A1	6.27 ± 1.28	5.61 ± 0.43	5.56 ± 1.12
M1	8.12 ± 1.41	6.85 ± 1.34	8.82 ± 1.19
P1	6.49 ± 1.75	6.18 ± 0.98	6.2 ± 1.4
2. Wall area (mm^2)			
A1	2.39 ± 1.6 *, #	1.42 ± 0.43	1.72 ± 0.74
M1	4.4 ± 2.33	2.85 ± 1.75	3.29 ± 1.15
P1	3.16 ± 1.96 #	2.22 ± 1.8	2.17 ± 0.92
3. Luminal area (mm^2)			
A1	1.67 ± 1.62	1.07 ± 0.67	1.95 ± 0.82
M1	3.02 ± 2.17 ***	2.04 ± 1 ***	5.6 ± 1.44
P1	2.71 ± 1.26	2.19 ± 0.76	2.97 ± 1.18

*$p < 0.05$ **$p < 0.01$ ***$p < 0.001$ when compared with control. #$p < 0.05$ when compared with contralateral lesion. A1; A1 segment of anterior cerebral artery, M1; M1 segment of middle cerebral artery, P1; P1 segment of posterior cerebral artery.

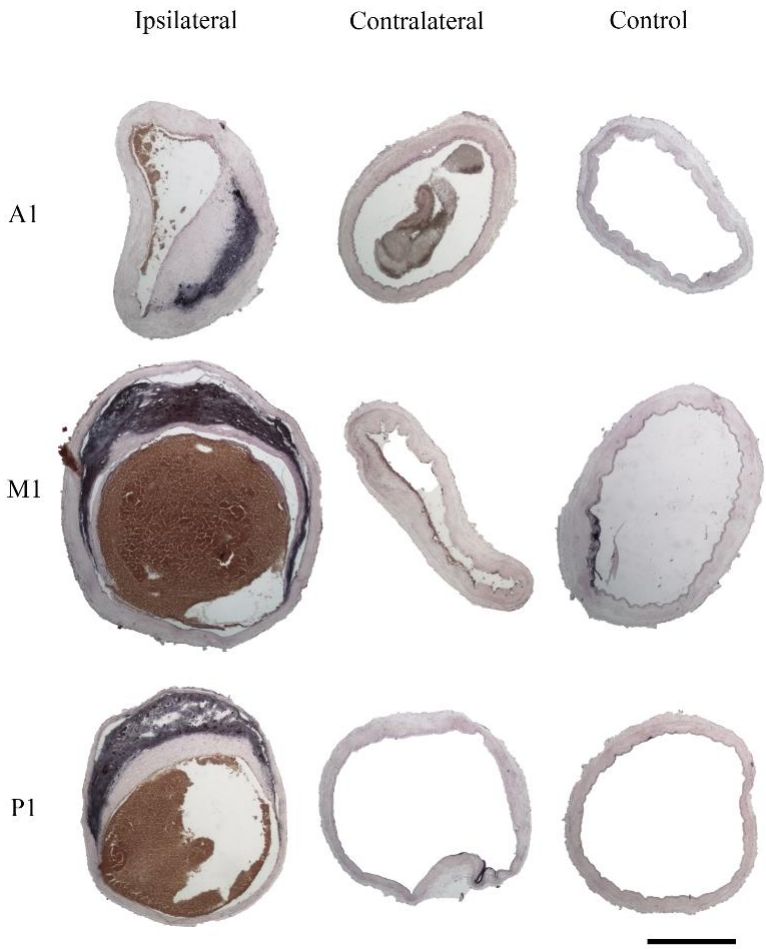

Figure 2 The Sudan black B-stained cross-sectional vessels of the A1 (S630702), M1 (S630801), and P1 (S630702) ipsilateral to hemorrhage and the A1(S621001), M1 (S631101), and P1 (S630302) contralateral to hemorrhage, and those of the control A1 (C630901), M1(C630902), and P1 (C630901). The scale bar is 1 mm.

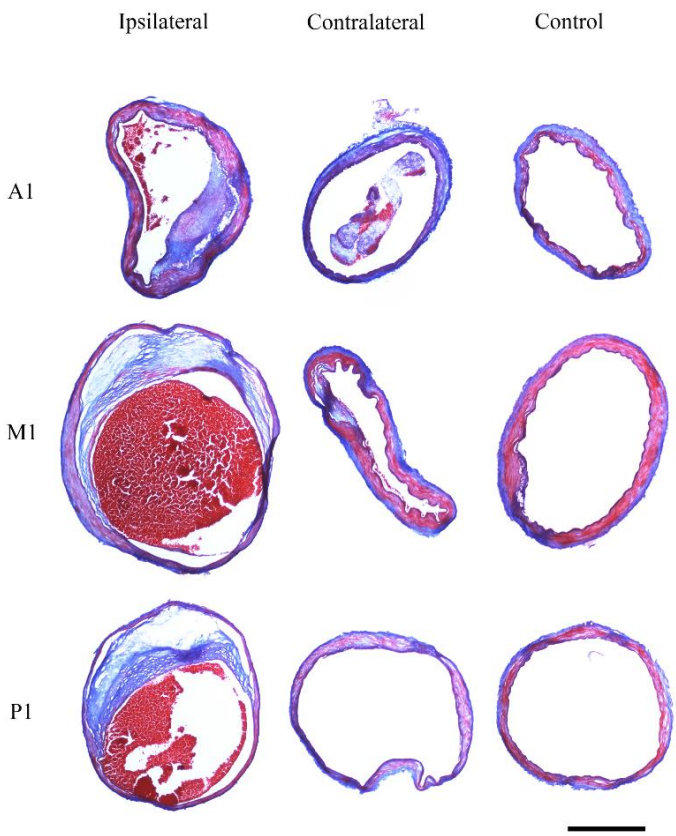

Figure 3 The Trichrome-stained cross-sectional vessels of the A1 (S630702), M1 (S630801), and P1 (S630702) ipsilateral to hemorrhage and the A1(S621001), M1 (S631101), and P1 (S630302) contralateral to hemorrhage, and those of the control A1 (C630901), M1(C630902), and P1 (C630901). The scale bar is 1 mm.

Table 2 The vascular parameters of ipsilateral and contralateral lesion of A1, M1, and P1 in hemorrhagic stroke cadavers and those of the control

Parameters	Ipsilateral	Contralateral	Control
1. Area of lipid (mm^2)			
A1	0.35 ± 0.72	0.07 ± 0.07	0.12 ± 0.12
M1	1.72 ± 1.4 $^{*,\#}$	0.41 ± 0.49	0.55 ± 0.6
P1	0.77 ± 0.84	0.08 ± 0.09	0.31 ± 0.44
2. Area of collagen (mm^2)			
A1	1.77 ± 1.04	1.42 ± 0.51	1.46 ± 0.72
M1	3.25 ± 1.13 **	2.58 ± 1.09	2.29 ± 0.76
P1	2.24 ± 1.13	1.72 ± 1.26	1.66 ± 0.56
3. Color intensity of elastin (value)			
A1	149.71 ± 40.41 **	141.89 ± 15.53	123.55 ± 27.71
M1	154.32 ± 19.3 ***	150.15 ± 19.39 ***	104.96 ± 23.79
P1	144.63 ± 24.54 **	130.74 ± 4.52	114.82 ± 31

*$p < 0.05$ **$p < 0.01$ ***$p < 0.001$ when compared with control. $^{\#}p < 0.05$ when compared with contralateral lesion. A1; A1 segment of anterior cerebral artery, M1; M1 segment of middle cerebral artery, P1; P1 segment of posterior cerebral artery.

4.2 Lipids, collagen, and elastin content changing in hemorrhagic cerebral artery

The deposits of lipids in the vessel were detected by SBB staining, as shown in Figure 2. The black stained lipid area was located inside the unevenly thickened wall regions, which were relatively empty areas, as shown in the H&E-stained sections. The areas of lipid deposits in the ipsilateral A1, M1, and P1 were found to vary in size. The lipid area is seen as a sheath inside the double layered wall. The cross-sectional ipsilateral M1 had the largest lipid area (1.72 ± 1.4 mm^2) among those of the contralateral (0.41 ± 0.49 mm^2) and control (0.55 ± 0.6 mm^2) M1 as shown in Table 2. However, there were no differences in the deposited lipid areas among the ipsilateral, contralateral, control A1, and those of P1.

Figure 3 displays the collagen fibers, smooth muscle fibers, and nuclei in the vascular wall using trichrome staining. There were different patterns of the collagen deposits in the cerebral artery among the ipsilateral, contralateral, and control vessels. In the control groups, the blue-stained collagen fibers were distinctly located in the tunica adventitia. However, they were found to be distributed into the tunica media of the contralateral vessel and appeared to be accumulating in the subendothelial layer of the uneven thickening wall of the ipsilateral vessels. The area of collagen fibers in the ipsilateral M1 wall (3.25 ± 1.13 mm^2) was significantly larger than that of the control (2.29 ± 0.76 mm^2), as shown in Table 2. The red-stained smooth muscle fibers were densely positioned in the tunica media of the control vessel but were loosely arranged and mixed with the collagen fibers in both the tunica media and subendothelial layer of the contralateral and ipsilateral vessels. There were empty spaces between two layers of the mixed collagen and smooth muscle fibers in all ipsilateral cerebral arteries.

The elastic fibers of the internal elastic lamina were revealed as black stained waving lines using a modified Verhoeff's Van Gieson/ EVG staining. Figure 4 shows that the internal elastic lamina was located close to the endothelial layer, whereas the red-stained collagen fibers were located in the tunica adventitia and the yellow red-stained muscle fibers were clearly located in the tunica media of the control vessels. The internal elastic lamina was seen as a regular wavy line surrounding the luminal surface of the control A1, M1, and P1. The external elastic lamina was also identified in the tunica adventitia of the control vessels. However, in the ipsilateral vessels, the internal elastic lamina is indicated by light black stained unwavering lines. These lines were noticeable on the thickening part of the vascular wall.

As shown in Table 2, the value of the color intensity of the internal elastic lamina in the ipsilateral A1(149.71 ± 40.41), M1(154.32 ± 19.3), and P1 (144.63 ± 24.54) were significantly higher than those of the control A1 (123.55 ± 27.71), M1 (104.96 ± 23.79), and P1(114.82 ± 31), respectively. That value of the contralateral M1 was significantly higher than that of the control. These values suggest that the ipsilateral A1, M1, and P1 and the contralateral M1 had significantly fewer elastic fibers than their corresponding control vessels.

4.3 Histological changes in the hemorrhagic nervous tissue

The nervous parenchyma of the hemorrhagic lesion had been damaged as seen in Figure 5a. Neither the gray or white matter could be identified because it was mostly filled with blood. Figure 5b shows the brain tissue contralateral to the hemorrhagic hemisphere. The gray matter and white matter of that brain tissue can be observed but the texture of brain tissue was inhomogeneous. There were numerous spaces in the gray matter and between the nerve fibers in the white matter of the contralateral brain tissue.

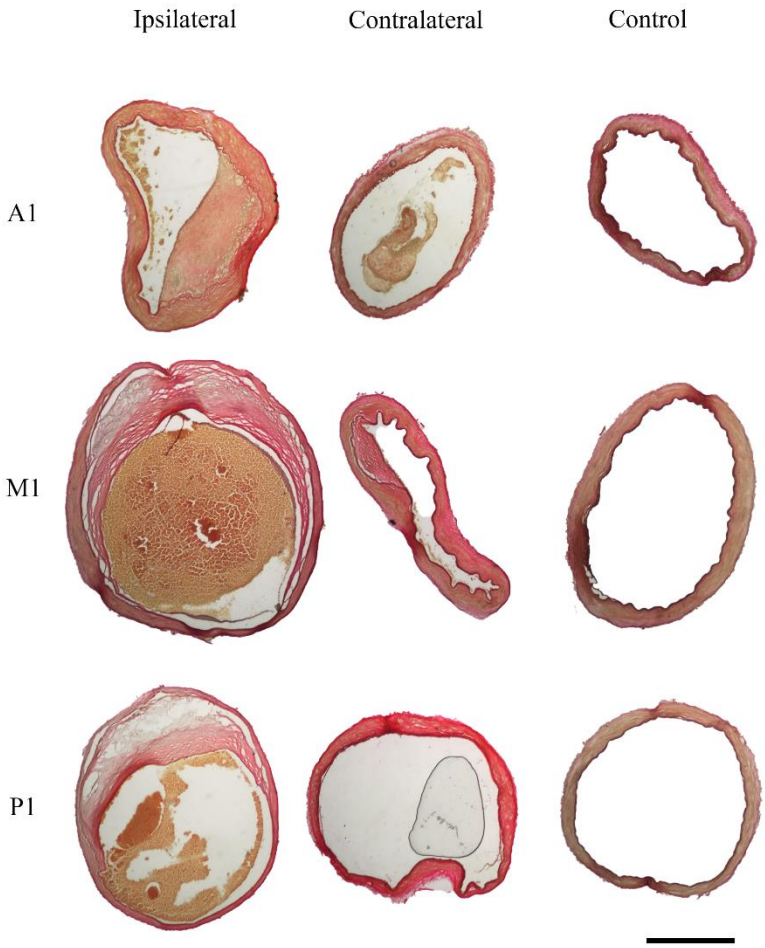

Figure 4 The Verhoeff's Van Gieson-stained cross-sectional vessels of the A1 (S630702), M1 (S630801), and P1 (S630702) ipsilateral to hemorrhage and the A1(S621001), M1 (S631101), and P1 (S630302) contralateral to hemorrhage, and those of the control A1 (C630901), M1(C630902), and P1 (C630901). The scale bar is 1 mm.

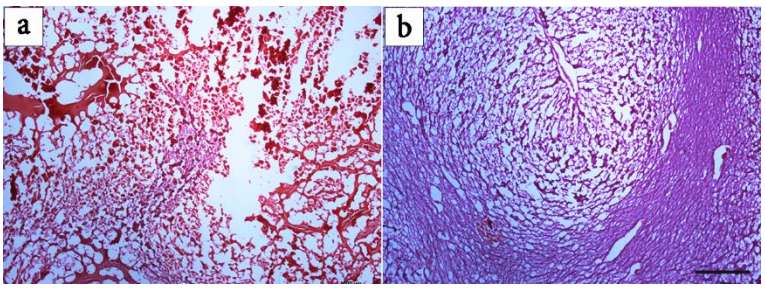

Figure 5 The nervous parenchyma from the hemorrhagic lesion; S621101 (a), contralateral to the hemorrhage lesion; S621101 (b). The scale bar in b is 1 mm and is applied to figure a.

5. Discussion

The samples in this study were from cadavers with ages of mostly over 60 years. All cerebral artery segments ipsilateral to the hemorrhagic lesion demonstrated atherosclerosis. A previous study also reported that cerebral artery from the elderly averaging over 60 years showed a tendency to have cerebral atherosclerosis (Enache et al., 2012). In addition to having atherosclerosis, the cerebral vessels in the elderly were significantly smaller than those in younger individuals (Hassan et al., 2020). The data of the vascular parameters such as the luminal perimeter, wall area, and luminal area between the A1, M1 and P1 ipsilateral and those of contralateral to the hemorrhagic lesion were reported in this study. However, approximately 30 % of the anatomical variation was found in the A1 segment (Gunnal, Wabale, & Farooqui, 2013).

The normal diameter of the M1 segment is relatively larger than that of the A1 and P1, respectively (Hassan et al., 2020). However, our study found that the luminal area of MI segment, both ipsilateral and contralateral to the hemorrhagic lesion, demonstrated the most reduction from the control size when compared to the other segments. A postmortem study reported that the middle cerebral artery had the most severe narrowing among arteries of the cerebral circulation (Yang et al., 2017). Previous reports mentioned that a stenosis in the middle cerebral artery could lead to stroke (Chandra et al., 2017). The arterial stenosis occurred by endothelial damage (Della-Morte, & Rundex, 2015). The H&E staining of the atheromatous plaque in this study showed poor staining of the core lipid, as previous studies have also noted (Yang et al., 2017; Enache et al., 2012; Pleşea et al., 2005). We used the Sudan black B stain to identify the core lipid component which were covered by the collagenous layer called the fibrous cap. A trichrome stain was used to identify the collagen fibers and smooth muscles cells and the modified Verhoeff's Van Gieson was used to review the elastic fibers, especially the internal elastic lamina. Since we had considered the particular benefits of these three staining methods, we were able to measure the vascular lipids, collagens, and internal elastic lamina effectively. In this study, the ipsilateral M1 segments demonstrated the highest lipid and collagen components compared to those of the contralateral side to the hemorrhagic lesion and the control. The internal elastic laminar density in the ipsilateral P1, M1, and P1 segments was significantly reduced from that of the control. The amount of the core lipid was varied and caused various sizes of atheromatous plaque in part of the arterial wall as reported in a previous study (Pleşea et al., 2005). The lipid accumulated in the subendothelial layer due to the presence of low-density lipoproteins (LDLs) entering after the endothelial damage had taken place (Weber and Noels, 2011). Macrophages were detected for their distribution in the atheromatous plaque (Yang et al., 2017) to phagocytose the LDL. These indicated that an inflammation had occurred in the plaque (Chandra et al., 2017).

We noticed that the tunica media of the ipsilateral arteries were unevenly thick along the circular wall. The tunica media in the wall region without the plague was obviously thinner than the part containing the plaque. This resulted from the smooth muscles in the tunica media being drawn into the tunica intima by the cytokine released from the inflammation (Chandra et al., 2017). The collagen fibers were also highly deposited in the subendothelial layer of the ipsilateral vessels lesion. The collagen fibers were found to be a major component of the plaque and have complicated roles relating to the smooth muscle cells and the inflammatory process itself (Adiguzel et al., 2009).

The contralateral nervous parenchyma demonstrated a minor defect, being likely edema or inflammatory parenchyma. These phenomena might have resulted from the brain parenchymal lysis due to the delay between the time of death and the collection of the brain. However, this needs to be compared with normal parenchymal tissue collected from the same region as the hemorrhagic lesion.

6. Conclusion

The A1 and P1 segments, as well as the M1 segments ipsilateral to the hemorrhagic hemisphere demonstrate significant morphological changes in terms of their wall areas and luminal area, respectively. Upon comparing the contents in the vessels, it was determined that major changes in lipid and collagen were found only in the wall of M1 segment ipsilateral to the hemorrhagic hemisphere, while major changes in elastin were found in all segments. Using special stains for vascular lipids, collagen, and elastic fibers, this study revealed comparative data for these components found in the ipsilateral, contralateral, and control vessels.

However, further investigation is needed regarding the immunohistochemical study that detects microglia in the nervous parenchyma, macrophages in the atheromatous plaque, and the endothelium of the A1, M1, and P1 segments.

7. Acknowledgements

The authors would like to thank the Neuromuscular Laboratory, the Plastination & Neurobiology Laboratory, and the Histology laboratory, Faculty of Medicine, Chiang Mai University for grant support (grant number 064-2563) and use of these facilities.

8. References

Adiguzel, E., Ahmad, P., Franco, C., & Bendeck, M. P. (2009). Collagens in the progression and complications of atherosclerosis. *Vascular Medicine, 14*(1), 73-89.

Chandra, A., Li, W. A., Stone, C. R., Geng, X., & Ding. Y. (2017). The cerebral circulation and cerebrovascular disease I: Anatomy. *Brain circulation, 3*(2), 45-56.

Chandra, A., Stone, C. R., Li, W. A., Geng, X., & Ding, Y. (2017). The cerebral circulation and cerebrovascular disease II: Pathogenesis of cerebrovascular disease. *Brain circulation, 3*(2), 57-65.

Della-Morte, D., & Rundex, T. (2015). The role of shear stress and arteriogenesis in maintaining vascular homeostasis and preventing cerebral atherosclerosis. *Brain circulation, 1*, 53-62.

Enache, A. L., et al. (2012). Histological and immunohistochemical aspects of cerebral vessels of the elderly. *Romanian Journal of Morphology and Embryology*, *53*(4), 1043-1050.

Gerrits, P. O., Brekelmans-Bartels, M., Mast, L., Gravenmade, E. J., Horobin, R.W., Holstege, G. (1992). Staining myelin and myelin-like degradation products in the spinal cords of Chronic Experimental Allergic Encephalomyelitis (Cr-EAE) rats using Sudan black B staining of glycol methacrylate-embedded material. *Journal of Neuroscience Methods*, *45*(1), 99-105.

Gorelick, P. B., Wong, K. S., Bae, H. J., & Pandey, D. K. (2008). Large artery intracranial occlusive disease: a large worldwide burden but a relatively neglected frontier. *Stroke, 39*(8), 2396-2399.

Gunnal, S. A., Wabale, R. N., & Farooqui, M. S. (2013). Variations of anterior cerebral artery in human cadavers. *Neurology Asia, 18*(3), 249-259.

Hassan, H. N., Mansor, M. A. E-B., Ibrahim, A. A. S., & Ibrahim, I. H. (2020). Anatomical measurements of cerebral arteries using digital subtraction angiography. *Ain Shama Medical Journal, 71*(2), 259-267.

Javed, K., Reddy, V., & Das J. M. (2022, July). *Neuroanatomy, Posterior Cerebral Arteries*. StatPearls [Internet]. Retrieved from https://www.ncbi.nlm.nih.gov/books/NBK538474/

Kim, J. S., Kang, D-W., $ Kwon, U. (2005). Intracranial arthrosclerosis: Incidence, Diagnosis and Treatment. *Journal of Clinical Neurology, 1*(1), 1-7.

Pleşea, I. E., Cameniţă, A., Georgescu, C. C., Enache, S. D., Zaharia, B., Georgescu, C. V., Tenovici, M. (2005). Study of cerebral vascular structures in hypertensive intracerebral haemorrhage. *Romanian Journal of Morphology and Embryology, 46*(3), 249-256.

Thaweekhotr, P., Thongsopha, C., Tanprawate, S., Sudwan, P., Bumroongkit, K., .. & Quiggins, R. (2022). Incidence of death from stroke and brains of stroke victim cadavers in Northern Thailand. *Chiang Mai University Journal of Natural Science, 21*(2), Article e2022028. https://doi.org/10.12982/CMUJNS.2022.028

Weber, C., &Noels, H. (2011). "Atherosclerosis: current pathogenesis and therapeutic options. *Nature medicine, 17*(11), 1410-1422.

Yang, W. J., Zheng, F., Niu, C. B., Paganini-Hill, A., Zhao, H. L.,… Chen, X. Y. (2017). Histological characteristics of intracranial atherosclerosis in a Chinese population: A postmortem study. *Frontiers in Neurology, 8*, Article 488. https://doi.org/10.3389/fneur.2017.00488